ELSEVIER

Biochimica et Biophysica Acta 1417 (1999) 89–100

BIOCHIMICA ET BIOPHYSICA ACTA

BBA

Maximum solubility of cholesterol in phosphatidylcholine and phosphatidylethanolamine bilayers

Juyang Huang, Jeffrey T. Buboltz, Gerald W. Feigenson *

Section of Biochemistry, Molecular and Cell Biology, Cornell University, 201 Biotechnology Building, Ithaca, NY 14853, USA

Received 9 October 1998; received in revised form 21 December 1998; accepted 21 December 1998

Abstract

In any lipid bilayer membrane, there is an upper limit on the cholesterol concentration that can be accommodated within the bilayer structure; excess cholesterol will precipitate as crystals of pure cholesterol monohydrate. This cholesterol solubility limit is a well-defined quantity. It is a first-order phase boundary in the phospholipid/cholesterol phase diagram. There are many different solubility limits in the literature, but no clear picture has emerged that can unify the disparate results. We have studied the effects that different sample preparation methods can have on the apparent experimental solubility limit. We find that artifactual demixing of cholesterol can occur during conventional sample preparation and that this demixed cholesterol may produce artifactual cholesterol crystals. Therefore, phospholipid/cholesterol suspensions which are prepared by conventional methods may manifest variable, falsely low cholesterol solubility limits. We have developed two novel preparative methods which are specifically designed to prevent demixing during sample preparation. For detection of the cholesterol crystals, X-ray diffraction has proven to be quantitative and highly sensitive. Experiments based on these methods yield reproducible and precise cholesterol solubility limits: 66 mol% for phosphatidylcholine (PC) bilayers and 51 mol% for phosphatidylethanolamine (PE) bilayers. We present evidence that these are true, equilibrium values. In contrast to the dramatic headgroup effect (PC vs. PE), acyl chain variations had no effect on the cholesterol solubility limit in four different PC/cholesterol mixtures.

Keywords: Liposome preparation; Cholesterol monohydrate; Cholesterol crystal; Demixing; X-ray diffraction

1. Introduction

Most eukaryotic cells contain membrane sterols and all vertebrates synthesize cholesterol [1]. In mammalian cells, as much as 90% of all cholesterol can be found in the plasma membrane [2]. Estimates of the cholesterol content in animal cell plasma membranes have ranged between 25 mol% and 50 mol% [1], implying that the interactions between cholesterol and other membrane components (including other cholesterols) might play a central role in establishing the properties of the membrane.

Because pure cholesterol cannot form a bilayer, there must be an upper limit on the cholesterol concentration that can be accommodated within any phospholipid bilayer. Any excess cholesterol will tend to precipitate from the membrane as crystals of pure cholesterol monohydrate. This cholesterol solubility limit is a well-defined quantity: a first-order phase boundary in the phospholipid/cholester-

* Corresponding author. Fax: +1-607-255-2428; E-mail: gwf3@cornell.edu

0005-2736/99/$ – see front matter
PII: S0005-2736(98)00260-0

ol thermodynamic phase diagram. Determining this limit for a systematic series of phospholipid/cholesterol mixtures would inform studies on the nature of phospholipid–cholesterol interactions. Many researchers have sought to measure this solubility limit in a number of model systems [3–12] and though there is no shortage of published work on the subject, no clear picture has emerged which can unify the disparate observations.

In principle, this solubility limit should be straightforward to determine: bilayer suspensions of increasing cholesterol content are prepared and each sample examined to determine the critical mole fraction of cholesterol at which crystals begin to form. In the initial stages of this study, we found that several methods (e.g., 90° light scattering, X-ray diffraction, ultrafiltration) could be used effectively to determine the point at which cholesterol crystals appear in different phospholipid mixtures. But regardless of which detection method we used, it became clear that the reproducibility of these 'straightforward' solubility limits was surprisingly poor. We were gradually forced to conclude that the source of this variability was heterogeneity in the samples themselves, caused by demixing between components during sample preparation. Indeed, Davis has reported difficulty in preparing homogeneous suspensions of phospholipid/cholesterol mixtures [13], and it has long been suggested that artifacts arising from sample preparation could explain the confusion which surrounds cholesterol solubility limits in bilayers [6,7].

In this study, we report the determination of solubility limits for four different phosphatidylcholine (PC)/cholesterol mixtures and one phosphatidylethanolamine (PE)/cholesterol mixture. For all of the PC/cholesterol mixtures, these solubility limits are essentially indistinguishable, falling near 66 mol% cholesterol. In stark contrast, the cholesterol solubility limit in a phosphatidylethanolamine bilayer is only about 51 mol%. We will present evidence that these are the true, equilibrium solubility limits for cholesterol in each of these bilayers. Phospholipid/cholesterol demixing artifacts, which can obscure the true solubility limit in conventionally prepared samples, will be discussed as will two independent preparative methods which we have developed to avoid these artifacts.

2. Materials and methods

Phospholipids were purchased from Avanti Polar Lipids (Alabaster, AL), cholesterol from Nu Chek Prep (Elysian, MN). Purity ($>99\%$) was confirmed by thin layer chromatography on washed, activated silica gel plates (Alltech Associates, Deerfield, IL), developing with chloroform/methanol/water = 65:25:4 for phospholipid analysis or with petroleum ether/ethyl ether/chloroform = 7:3:3 for cholesterol analysis. All solvents used were of HPLC grade. TLC plates were quantitated by charring and densitometry. Phospholipid stock solutions were quantitated by phosphate assay [14]. Aqueous buffer (pH 7.0, 5 mM PIPES, 200 mM KCl) was prepared from purified water (Milli-Q system, Millipore) and filtered through a 0.1 μm filter before use. FEP Teflon Oak Ridge centrifuge tubes were purchased from Nalge Company. One-mm, special glass X-ray capillaries were purchased from Charles Supper (Natick, MA).

2.1. Liposome preparations

2.1.1. Film deposition

Components were codissolved in $CHCl_3$ and bulk solvent removed under a gentle stream of nitrogen gas, depositing a lipid film on the surface of a test tube. Any remaining solvent residue was removed by vacuum incubation for $\sim$10 h at a measured pressure of $\sim$30 mTorr. Deposited films were hydrated in aqueous buffer at room temperature and dispersed by vortexing for 1 min. Samples containing di16:0-PC were hydrated and vortexed at 50°C, before being cooled slowly to room temperature. All samples were sealed under argon after hydration.

2.1.2. Lyophilization

Components were codissolved in cyclohexane/methanol, 99:1, and this solution was frozen in liquid nitrogen. The sample was placed in a vacuum desiccator on water ice and bulk solvent was removed by sublimation under vacuum. After bulk solvent had been removed, the desiccator was warmed to room temperature and the vacuum incubation was continued for $\sim$10 h at $\sim$30 mTorr. The voluminous lipid powders were hydrated, vortexed and sealed under argon in the same manner as the films.

2.1.3. Rapid solvent exchange (RSE)

This method has recently been described in detail elsewhere [15]. Briefly, lipids were codissolved in 10–100 μl of dichloromethane (0.1% MeOH, 0.05% H_2O) and then sprayed into vortexing buffer at reduced pressure, rapidly vaporizing the solvent and precipitating the lipid mixture in an aqueous environment. For sample preparation of mixtures containing di16:0-PC, the buffer was maintained at 50°C throughout the RSE procedure, before cooling to room temperature. All samples were sealed under argon immediately following RSE.

2.1.4. Low-temperature trapping (LTT)

This method will soon be described in detail elsewhere (Huang and Feigenson, in preparation). Lipids were dissolved in $CHCl_3$ and the solvent removed under vacuum at ~30 mTorr for ~10 h. Lipids were re-dissolved in dry chloroform containing 1% methanol, then frozen in liquid nitrogen. Samples were lyophilized at low temperature, carefully controlling the temperature so that the chloroform remains solid. After bulk solvent had been removed, the lipid powders were kept cool (−20°C) during continued vacuum incubation (~12 h) to remove residual solvent. Just before hydration, the sample was warmed to room temperature in a stirring water bath for 1 min, then buffer added to the dry powder. The suspension was immediately vortexed for 1 min. Samples containing di16:0-PC were hydrated and vortexed at 50°C. All samples were sealed under argon following hydration.

2.2. Cholesterol crystal detection

The measurements described below were all made at room temperature (23–25°C).

2.2.1. Optical microscopy

Optical microscopy was used to detect cholesterol crystals in lipid dispersions. A Zeiss IM35 microscope was used in either phase-contrast, brightfield, or polarized mode. A Nikon Fluor 100× and a 40× oil immersion objective were used. Typically, 10 μl of a 3-mM lipid dispersion was viewed on a thin coverglass. Images were captured and enhanced by a Dage MTI CCD-72 camera (Dage MTI, IN) and viewed on a video monitor.

2.2.2. Light scattering

Ninety-degree light scattering was measured using a Hitachi fluorescence spectrophotometer (model F-3010) interfaced to a Macintosh computer. Samples were illuminated at 500 nm (1.5-mm slit; 500-nm interference filter) with detection at 500 nm (1.5-mm slit). About 1.5 ml of a 100 μM suspension was added to a cuvette with a masked stirbar. Scattered light intensity was averaged over 1 min.

2.2.3. X-Ray diffraction

Hydrated liposome dispersions made by film deposition, lyophilization, or LTT were first pelleted at $1000\times g$ for 10–25 min; dispersions made by RSE were pelleted at $20\,000\times g$ for 15 min. The lipid sediment was loaded into thin-walled 1.0 mm glass X-ray capillaries and further centrifuged in a buoyant support apparatus [15] at $20\,000\times g$ for 15 min to produce a uniformly dense pellet. Typically, white lipid sediment filled the bottom 4–8 mm of the capillary, with clear buffer above. Capillaries were sealed by paraffin wax under argon gas. A typical sample contained about 1.5 mg of lipid.

X-Ray diffraction experiments were carried out at the A-1 and F-1 beamlines at the Macromolecular Diffraction Facility at the Cornell High Energy Synchrotron Source (MacCHESS). Samples were illuminated by an intense synchrotron X-ray beam, with a wavelength of 0.908 Å, passing through a 0.2-mm collimator. Diffraction images were collected with a Princeton 2K CCD detector containing 2048×2048 41-μm pixels [16,17]. At the sample-to-detector distance of 280 mm, the wide dynamic range (16 bits) and the resolution of the CCD detector allowed capture of both the low-angle and wide-angle diffraction patterns (from 3.8 Å to 110 Å) simultaneously on the same image. Depending on beam intensity and sample density, the exposure time for hydrated samples varied from 10 to 80 s; for dry samples, 0.5 to 3.0 s.

Capillaries were mounted in a sample holder coupled to a computer-controlled stepping-motor stage which could move vertically or horizontally, perpendicular to the beam. Samples were scanned 2–3 mm along the capillary axis during exposure, using the stepping motor. This procedure reduces radiation damage to the lipid and achieves more representative sampling.

Image files were corrected for geometric distor-

tions introduced by the CCD camera. To transform the powder patterns into radial profiles of diffraction intensity, each image was circularly integrated (using the IMP program [18] provided by CHESS). The center of the beam and the tilt angle of the detector surface were precisely determined to prevent line broadening. Diffraction peaks in Bragg spacing were calibrated using the $Ca(PS)_2$ line at 49.1 Å as a standard [19].

3. Results

3.1. Detection methods

We use the term χ^*_{chol} to refer to the critical bilayer mole fraction of cholesterol above which excess cholesterol precipitates as the monohydrate crystal. A variety of methods were used to determine this solubility limit; three of these are discussed below.

3.1.1. Light microscopy

The advantage of light microscopy is that cholesterol crystals and lipid vesicles can be identified by direct, visual observation. Each sample in a series is searched for crystals of cholesterol monohydrate, trying to determine the mole fraction of cholesterol above which cholesterol crystals are present. As a method for the determination of χ^*_{chol}, light microscopy was imperfect for three reasons. First, optical microscopy does not resolve crystals on a scale much smaller than 1 μm. Second, the quantity of crystals cannot be reliably estimated, due to variations in crystal size and thickness. Third, the nature of such a visual search makes it possible that cholesterol crystals will be missed in samples near χ^*_{chol}, even if multiple sample aliquots are examined. Therefore, light microscopy serves best as a supporting technique.

Cholesterol crystals were identified mainly by their shape using brightfield microscopy. Although cholesterol crystals have strong birefringence, polarized light microscopy was not very useful for our purpose. In samples of cholesterol content just above χ^*_{chol}, the number and sizes of crystals are usually small. Rotation of polarized light by crystals was very weak in these samples, whereas birefringence from the plentiful lipid vesicles overwhelmed the field of view.

3.1.2. 90° Light scattering

Determination of χ^*_{chol} by 90° light scattering exploits the differences in size, structure and refractive index between cholesterol crystals and bilayer vesicles. For many phospholipid/cholesterol mixtures, a sudden increase in signal intensity correlates with the appearance of cholesterol crystals by X-ray diffraction (data not shown). However, this method

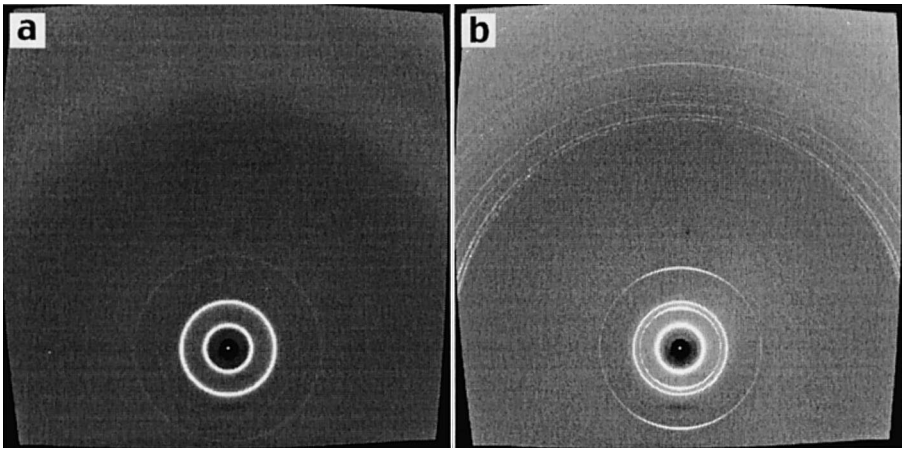

Fig. 1. X-Ray diffraction powder patterns for two di12:0-PC/cholesterol mixtures prepared by LTT: (a) with $\chi_{chol} = 0.60$, only lipid lamellar diffraction is detected; (b) with $\chi_{chol} = 0.73$, diffraction from lipid lamellae as well as from cholesterol monohydrate crystals is detected.

does not work well with all preparations. We found that light scattering did not reveal χ^{*}_{chol} in mixtures of cholesterol with 16:0,18:1-PE.

3.1.3. X-Ray diffraction

Fig. 1a shows an X-ray diffraction powder pattern for a di12:0-PC/cholesterol mixture with $\chi_{chol} = 0.60$. The two, low-angle concentric rings are the first- and the second-order lamellar repeats. The radial profile of diffraction intensity is shown in Fig. 2a; the peaks at 58.6 Å and 29.3 Å correspond to the first- and second-order lamellar repeats, respectively. The wide-angle data reveal a broad, diffuse peak centered at 4.85 Å, as shown in Fig. 2b.

Fig. 1b shows the powder pattern obtained for a di12:0-PC/cholesterol mixture with $\chi_{chol} = 0.73$. The cholesterol composition in this sample exceeds the maximum solubility of cholesterol in a di12:0-PC bilayer (see below). Therefore, in addition to lamellar phase lipid, this sample also shows the diffraction pattern characteristic of cholesterol monohydrate crystals [20,21]. The radial profile of diffraction intensity is shown in Fig. 2c. Peaks correspond to the main cholesterol monohydrate repeat at 33.94Å (first-order) and 16.97 Å (second-order). Hereafter, we will refer to these as the 34 Å and 17 Å peaks. In the wide-angle region (Fig. 2d), a number of sharp peaks are evident which are characteristic of cholesterol monohydrate, at spacings between 4 and 6 Å. A broad 4.85 Å peak, caused by lateral order within the bilayer (Fig. 2b), gradually weakens and disappears with increasing cholesterol crystal content. This would seem to indicate that accumulation of cholesterol crystals can somehow disrupt lateral packing within the bilayer.

An advantage of the X-ray diffraction detection method is that it yields separate, characteristic signals for lamellar phase lipid and cholesterol monohydrate. This also allows a quantitative measure of the amount of crystalline cholesterol in a sample, once a radial profile of diffraction intensity has been produced from the powder pattern. As Fig. 2c

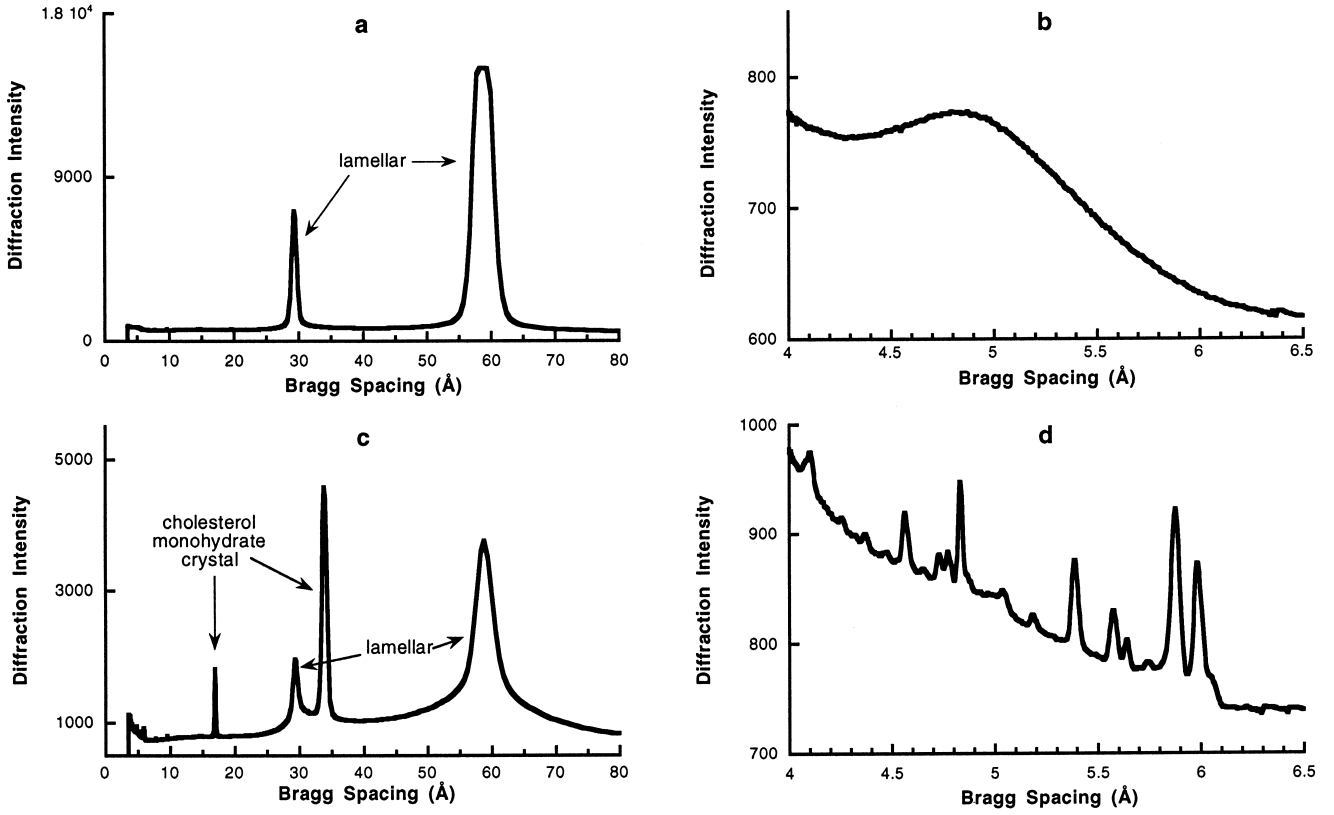

Fig. 2. Radial profiles of diffraction intensity for the mixtures shown in Fig. 1. (a,b) Low-angle and wide-angle diffraction for the sample shown in Fig. 1a; (c,d) low-angle and wide-angle diffraction for the sample shown in Fig. 1b.

shows, the quantity of cholesterol crystals can be assessed through integration of either the 34 Å, the 17 Å, or the wide-angle peaks between 4 and 6 Å. Although the 34 Å peak is the strongest, it often overlaps with the second-order lamellar-repeat peak. Therefore, we generally use the 17 Å peak as the quantitative indicator. This peak is sharp and the local background is relatively smooth and flat. We define the cholesterol crystal diffraction intensity I_c as

$$I_c = [I_a(16.5\ \text{Å}, 17.5\ \text{Å}) - I_{baseline}]/I_{beam} \quad (1)$$

where I_a(A,B) is the average diffraction intensity between A and B in Bragg spacing, $I_{baseline}$ is the background intensity near the 17 Å peak

$$I_{baseline} = [I_a(16.0\ \text{Å}, 16.5\ \text{Å}) + I_a(17.5\ \text{Å}, 18\ \text{Å})]/2 \quad (2)$$

and I_{beam} is an exposure factor

$$I_{beam} = I_a(90\ \text{Å}, 100\ \text{Å}) \quad (3)$$

The major sources of noise in I_c were from nonrepresentative sampling and inconsistent sample density. The signal-to-noise ratio was significantly improved by scanning the samples during exposure, and by pelleting samples in the capillaries with high speed centrifugation.

3.2. Sample preparation and equilibrium

3.2.1. Variable results by two conventional preparation methods

In sets of samples prepared by either film deposition or lyophilization, each individual experiment yielded an apparent χ^*_{chol} value. Unfortunately, the reproducibility between experiments was surprisingly poor (Table 1), and this variability far exceeded the uncertainty in the experimental measurements. For example, 26 separate experiments were performed on 16:0,18:1-PC/cholesterol mixtures prepared by lyophilization, and the apparent χ^*_{chol} values ranged from 51–65 mol% cholesterol.

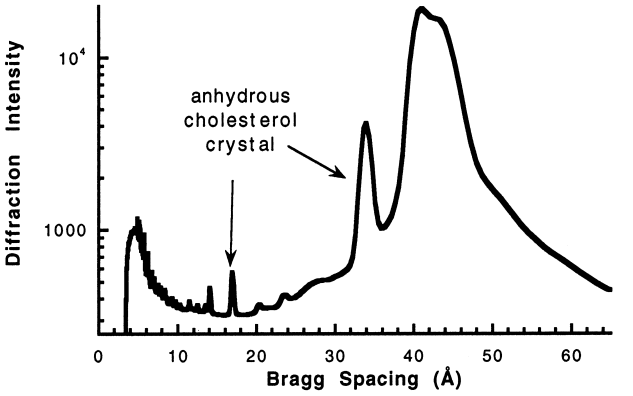

Fig. 3. Radial profile of X-ray diffraction intensity of a 16:0,18:1-PC/cholesterol deposited film, at $\chi_{chol} = 0.60$. Peaks correspond to dry lipid lamellae, as well as to anhydrous cholesterol crystals.

3.2.2. Artifactual cholesterol demixing

Fig. 3 shows the radial profile of diffraction intensity of a 16:0,18:1-PC/cholesterol deposited film, at $\chi_{chol} = 0.60$, on a semi-logarithmic scale. This pattern shows a set of lamellar repeats together with a set of peaks which correspond to anhydrous cholesterol crystals [22]. This confirms that some cholesterol has demixed from the phospholipid, forming crystals of pure cholesterol. Fig. 4 shows the 17 Å diffraction intensity due to anhydrous cholesterol crystals as a function of cholesterol content for a set of 16:0,18:1-PC/cholesterol deposited films. In this set of samples, anhydrous cholesterol crystals are present in every sample for which $\chi_{chol} > 0.45$.

Fig. 5 (squares) shows cholesterol crystal diffraction intensity (I_c in Eq. 1), from cholesterol monohydrate vs. χ_{chol} for a set of 16:0,18:1-PC/cholesterol mixtures which were hydrated from deposited films. After hydration, each sample was vortexed for 2 min. The dispersions were incubated at room temperature for 7 days, with 2 min of vortexing each day, before being transferred to capillaries and subjected to

Table 1
Variable, apparent cholesterol solubility limits observed in PC bilayers prepared by conventional preparation methods

Bilayer type	Range of apparent solubility limits by film deposition	Range of apparent solubility limits by lyophilization
16:0,18:1-PC	0.55–0.63	0.51–0.65
di16:0-PC	0.45–0.57	0.50–0.56

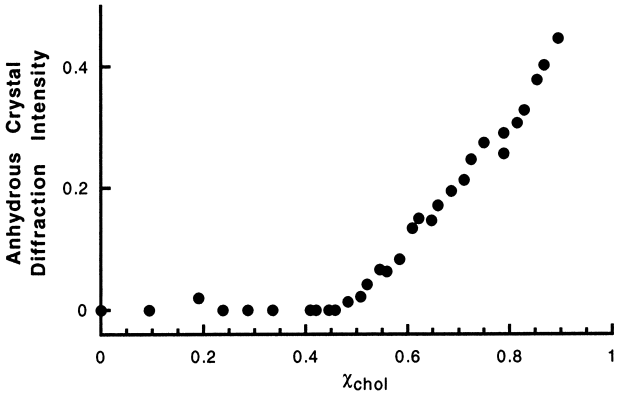

Fig. 4. Anhydrous crystal X-ray diffraction intensity vs. cholesterol mole fraction for a set of 16:0,18:1-PC/cholesterol deposited films.

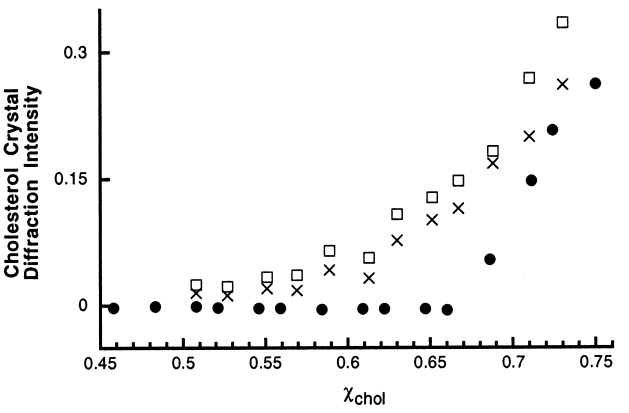

Fig. 5. Cholesterol monohydrate crystal diffraction intensity vs. cholesterol mole fraction for fully hydrated 16:0,18:1-PC/cholesterol mixtures. □, A set of samples prepared by film deposition method, 7 days after hydration; ×, the same sample set after 10 weeks of incubation at room temperature; ●, a set of samples prepared by LTT, 3 days after hydration.

X-ray diffraction. Although the true, equilibrium χ^*_{chol} value is 0.66 (see Section 4), cholesterol crystals were detected in samples with χ_{chol} as low as 0.51. The same samples were examined again after incubating them at room temperature for 10 weeks further. As shown in Fig. 5 (crosses), cholesterol crystal levels were slightly reduced, indicating that some cholesterol from the crystals had remixed with the lamellar phase lipid. Therefore, we sought to determine whether mechanical stirring or heating might accelerate remixing. Two identical sets of 16:0,18:1-PC/cholesterol dispersions were prepared by lyophilization and examined by light microscopy. Initially, the apparent χ^*_{chol} value was 0.52 for each set. The sample sets were then incubated under argon, at either 24°C or 45°C, with each sample constantly agitated by a small stirbar. Samples were flushed with argon and resealed every 3 days. After 1 month of incubation, the sample sets were re-examined by light microscopy. The apparent χ^*_{chol} values had increased to about 0.57 or 0.60 for the sample sets incubated at 24°C and 45°C, respectively. The lipid was extracted and examined by TLC, and no significant breakdown was found.

Table 2
Maximum solubility of cholesterol (χ^*_{chol}) in PC and PE bilayers, as determined in samples prepared by either RSE or LTT

Bilayer type	Solubility limit by RSE	Solubility limit by LTT
16:0,18:1-PC	0.66 (±0.01)	0.66 (±0.01)
16:0,18:1-PE	0.51 (±0.01)	0.51 (±0.01)
di22:1-PC	0.66 (±0.01)	0.66 (±0.01)
di12:0-PC	0.66 (±0.01)	0.66 (±0.01)
di16:0-PC	0.66 (±0.01)	0.66 (±0.01)

Although the majority of anhydrous cholesterol crystals were converted to monohydrate crystals after hydration, traces of anhydrous crystals were found in many of the mixtures prepared by film deposition or lyophilization, days after hydration. It has been dem-

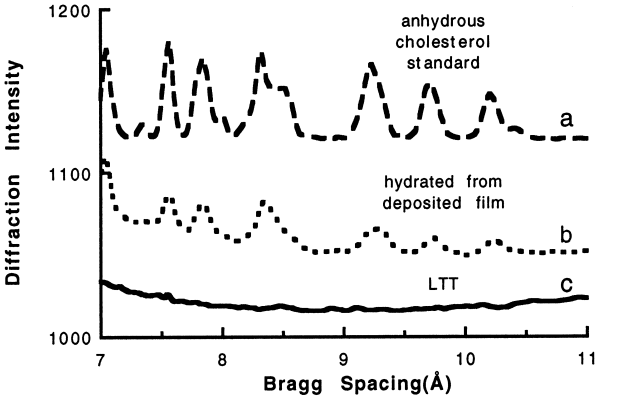

Fig. 6. Evidence of trace anhydrous cholesterol crystals in fully hydrated samples prepared by film deposition. (a) Diffraction intensity profile of anhydrous cholesterol crystals; (b) diffraction intensity of a 16:0,18:1-PC/cholesterol mixture with $\chi_{chol} = 0.70$, prepared by film deposition, 5 days after hydration; (c) 16:0,18:1-PC/cholesterol with $\chi_{chol} = 0.70$, prepared by LTT, 3 days after hydration.

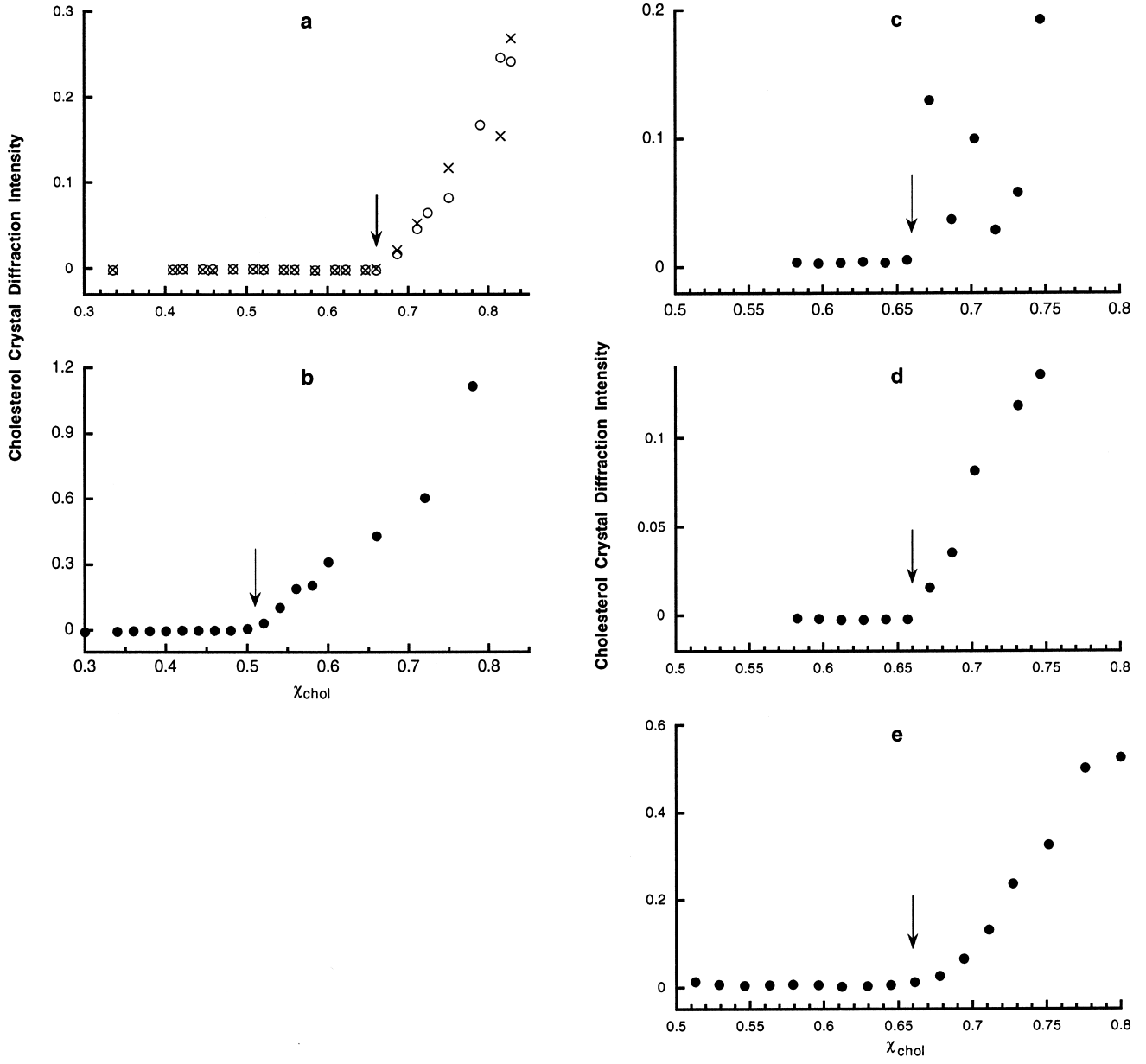

Fig. 7. Cholesterol monohydrate diffraction intensity (I_c in Eq. 1) vs. cholesterol mole fraction for several bilayer mixtures. Arrows indicate the average χ^*_{chol} value from at least three replicate experiments. (a) 16:0,18:1-PC/cholesterol mixtures prepared by LTT. ○, 3 days after hydration; ×, same sample set after 10 weeks incubation at room temperature. (b) 16:0,18:1-PE/cholesterol mixtures prepared by RSE. (c) di22:1-PC/cholesterol mixtures prepared by LTT. (d) di12:0-PC/cholesterol mixtures prepared by RSE. (e) di16:0-PC/cholesterol mixtures prepared by LTT.

onstrated that conversion from anhydrous cholesterol to the monohydrate is a slow process [20]. Fig. 6, trace b shows the radial profile of diffraction intensity for a 16:0,18:1-PC/cholesterol mixture, at $\chi_{chol} = 0.70$, hydrated from a deposited film. The wide-angle region between 7 and 11 Å in Bragg spacing is a good region to search for evidence of anhydrous cholesterol. In this region, there are no visible diffraction lines from either lipid lamellae or cholesterol monohydrate, but anhydrous cholesterol crystals show a series of sharp diffraction lines (Fig. 6, trace a). This sample has been hydrated five days, yet

the diffraction pattern clearly shows a set of peaks which correspond to anhydrous cholesterol. On the other hand, a sample prepared in parallel, from the same stock solution, by LTT shows no trace of anhydrous cholesterol (Fig. 6, trace c).

3.2.3. Reproducible solubility limits by novel preparative methods

Table 2 summarizes the results obtained in experiments based on the RSE and LTT methods of sample preparation. Each χ^*_{chol} value listed in this table is the result of at least three replicate experiments by each preparative method. In contrast to the results obtained by either film deposition or lyophilization, experiments based on RSE or LTT yield reproducible values of χ^*_{chol} which are, in every case, higher than the apparent χ^*_{chol} values in conventional preparations (Table 1 cf. Table 2). For every phospholipid/cholesterol mixture which we have examined so far, the same χ^*_{chol} value is obtained by both RSE and LTT. Sample sets prepared by RSE and LTT showed no change in the apparent solubility limit even over $\sim$10 weeks of incubation (Fig. 7a).

3.3. χ^*_{chol} Values for PC or PE bilayers

Simply exchanging the PC headgroup for a PE headgroup has a dramatic effect on the solubility limit, as shown in Fig. 7b. Cholesterol precipitates from bilayers of 16:0,18:1-PE at a cholesterol concentration 15 mol% lower than in bilayers of the PC analog. For the 16:0,18:1-PE bilayer, $\chi^*_{chol} = 0.51$ (± 0.01).

In contrast to the dramatic headgroup dependence, the cholesterol solubility limit in a PC bilayer seems to be insensitive to either increases or decreases in bilayer thickness, as revealed by cholesterol mixtures with di22:1-PC (Fig. 7c) or di12:0-PC (Fig. 7d). For each of these two bilayers, $\chi^*_{chol} = 0.66$ (± 0.01). The quantitative plots of crystal diffraction intensity were always more noisy for di22:1-PC/cholesterol mixtures than for other mixtures (Fig. 7c cf. Fig. 7a,b,d,e). This may be due to physical separation between lamellae and crystals during centrifugation, caused by the considerable density difference between cholesterol monohydrate and di22:1-PC vesicles. However, in every experiment on di22:1-PC/cholesterol, cholesterol monohydrate was only present in samples with $\chi^*_{chol} > 0.66$.

Unlike the three other PCs discussed so far, di16:0-PC forms gel-phase lamellae at room temperature. Nonetheless, at 24°C (Fig. 7e), the solubility limit of cholesterol in a di16:0-PC bilayer is indistinguishable from those observed in the other three PC mixtures: $\chi_{chol} = 0.66$ (± 0.01).

4. Discussion

The method of sample preparation is critical to the successful determination of true, equilibrium cholesterol solubility limits in phospholipid/cholesterol suspensions. Experiments based on either of two conventional preparative methods, film deposition or lyophilization, can produce apparent solubility limits which are not reproducible (Table 1). Both film deposition and lyophilization pass the phospholipid/cholesterol mixture through an intermediary solid state, either film or powder. Freeman and Finean reported that cholesterol crystals tend to precipitate from deposited films of egg PC and cholesterol [6]. Other workers have also observed the formation of pure cholesterol crystals in anhydrous lipid mixtures [23,24]. We have observed this phenomenon in several phospholipid mixtures, both in deposited films (Figs. 3 and 4) and lyophilized powders (data not shown). X-Ray diffraction identifies these cholesterol precipitates as crystals of anhydrous cholesterol, based on the characteristic diffraction lines, e.g., in the 7–11 Å region. Buboltz has proposed that the effects of solid-state demixing could persist in hydrated samples [15]. Indeed, after hydration, this demixed cholesterol is very slow to remix (Fig. 5) and transforms slowly to crystals of cholesterol monohydrate. Neither mechanical agitation nor heating, over several weeks' time, can bring about complete remixing of these artifactual crystals. The fact that the cholesterol crystals have some tendency to remix with the lamellar phase (Fig. 5) demonstrates that these samples are not at equilibrium, and that the true equilibrium value of χ^*_{chol} is higher than the apparent χ^*_{chol}. Overall, solid-state demixing of cholesterol during conventional sample preparation has the effect of producing variable, falsely low estimates of the cholesterol solubility limit. This may help to

explain the disparate χ^*_{chol} results that have been published in the literature [3–12].

The evidence we have presented demonstrates that phospholipid/cholesterol samples may not be at equilibrium when they are prepared by either film deposition or lyophilization. We have shown that nonequilibrium cholesterol crystals (both monohydrate and anhydrous) can be present in samples well below χ^*_{chol}. These particles of pure cholesterol have demixed from the lamellar phase lipid, which means that the actual cholesterol concentration in the bilayer must be lower than the nominal composition. The actual bilayer composition is unknown, and changes continuously as the nonequilibrium cholesterol crystals slowly remix with the lamellar phase.

Our attention has been focused on the true, maximum solubility limit of cholesterol in hydrated phospholipid lamellae. Our observations are limited to the regime of high cholesterol content (>35 mol%). We have been concerned with the formation of artifactual crystals of pure cholesterol, which represent an extreme of demixing. We have not examined phospholipid/cholesterol mixtures of lower cholesterol content and we have not sought any evidence of demixing which does not produce pure cholesterol crystals. In our opinion, it remains an unanswered question, whether less extreme forms of artifactual demixing can occur in phospholipid/cholesterol mixtures at lower cholesterol contents, or whether any such demixing would be reversible. For a discussion of the principles which may drive the demixing of components during conventional sample preparation, see Buboltz and Feigenson [15].

Cholesterol solubility limit experiments based on two novel preparative methods, RSE and LTT, seem to be free of demixing artifacts. These methods were designed to prevent demixing of lipids during sample preparation. Rapid solvent exchange does not pass the lipid mixture through an intermediary solid state, and so avoids any demixing that could be caused by complex solid-state phase behavior. In contrast, the strategy of low temperature trapping is to slow the kinetics of demixing. Mixtures are trapped in a well-mixed state by lyophilizing at low temperature. The following four points summarize our evidence that equilibrium results are obtained in experiments based on RSE or LTT. First, we could obtain reproducible χ^*_{chol} values by these preparative methods, but not by film deposition or lyophilization (Table 1 cf. Table 2). Second, these two new methods are very dissimilar, employing completely different strategies to prevent demixing, yet we obtain the same χ^*_{chol} values by either RSE or LTT (Table 2). Third, in every case, these solubility limits are higher than indicated by conventional preparations (Table 1 cf. Table 2), consistent with the elimination of a demixing artifact. Lastly, high cholesterol content bilayers prepared by RSE or LTT are stable. Even in samples which approach χ^*_{chol}, lamellar phase cholesterol remains in the bilayer and does not precipitate as crystals, even over prolonged incubation up to 10 weeks (Fig. 7). Based on these four observations, we conclude that χ^*_{chol} values obtained by both RSE and LTT are the true, equilibrium values. It may well be that other methods of sample preparation, not examined in this work, can likewise yield reproducible, equilibrium values of χ^*_{chol}.

It is notable that the true χ^*_{chol} values for PC or PE bilayers present a fairly simple picture. The headgroup effect is pronounced: exchanging a choline moiety for ethanolamine decreases the cholesterol solubility limit by about 15 mol%. In stark contrast, no acyl chain effect could be observed in four different PC/cholesterol mixtures. A di22:1-PC bilayer is nearly 40% thicker than a di12:0-PC bilayer [25], yet the χ^*_{chol} values are essentially identical in these two membranes. Nor is χ^*_{chol} different in di16:0-PC bilayers. Thus, at room temperature, the interactions which determine χ^*_{chol} do not depend on whether the PC would form a gel or fluid bilayer in its pure state.

Previously published cholesterol solubility limits have ranged between $\sim$0.33 and $\sim$0.66 for PC bilayers [5,7,26] and between 0.35 and 0.40 for PE bilayers [11]. These studies have generally employed film deposition. In each of the studies which have reported a maximum incorporation of 66 mol% cholesterol, the samples have been sonicated [5,6,8,27,28], whereas unsonicated preparations have generally produced lower apparent solubility limits of around 50 mol% cholesterol [3,4,6,8–10,29]. Some have concluded that the 66 mol% limit can only be achieved through sonication and is most likely a metastable state [6–8]. Our results clearly demonstrate that cholesterol may be stably incorporated up to 66 mol% in multilamellar PC bilayers

without sonication. Cholesterol does not precipitate from these cholesterol-rich multilamellar bilayers, even over 10 weeks of incubation at room temperature (Fig. 7a). The difference in apparent χ^*_{chol} values between unsonicated and sonicated (conventional) preparations may imply that sonication can remix demixed cholesterol with the lamellar phase, possibly by disrupting or destabilizing cholesterol crystals. However, we have not studied this issue and can only speculate.

It should be stressed that true, equilibrium values of χ^*_{chol} carry a clear and important thermodynamic meaning: at χ^*_{chol}, the chemical potential of cholesterol in the bilayer is equal to that of the monohydrate crystal, $\mu^{bilayer}_{chol} = \mu^{crystal}_{chol}$. This is because the chemical potential of cholesterol in crystals of pure cholesterol monohydrate is a constant, $\mu^{crystal}_{chol}$. On the other hand, the chemical potential of cholesterol in a lipid bilayer, $\mu^{bilayer}_{chol}(\chi_{chol})$, is a function of its bilayer concentration. When $\chi_{chol} \geq \chi^*_{chol}$, cholesterol-saturated lamellar phase coexists with cholesterol monohydrate. Therefore, χ^*_{chol} is the cholesterol mole fraction at which the chemical potential of lamellar phase cholesterol becomes equal to that of the monohydrate crystal, i.e., $\mu^{bilayer}_{chol} = \mu^*_{chol}$.

Such true, equilibrium values of χ^*_{chol} serve to compare the thermodynamics of mixing between cholesterol and other lipids in bilayers of different composition. In a Monte Carlo simulation study [30], we present a simple, microscopic interaction model of cholesterol–phospholipid mixing, containing a cholesterol multibody interaction term, which shows that the χ^*_{chol} values are most likely to occur near the discrete values of cholesterol concentration, 0.50, 0.57, and 0.67, corresponding to phospholipid to cholesterol ratios of 1/1, 3/4 and 1/2, respectively. At these solubility limits, where the chemical potential of cholesterol jumps steeply, cholesterol molecules form highly symmetrical regular distributions in bilayers. The physical origin of the multibody interaction might be related to the exposure of nonpolar cholesterol to water at high cholesterol concentration, i.e., the hydrophobic effect [30].

Acknowledgements

The authors would like to thank Dr. D. Thiel, Mr. B. Miller, Mr. C. Heaton and Dr. M. Szebenyi for help at CHESS. This work was supported by National Science Foundation Grant MCB-9722818. J.H. was supported, in part, by the W.M. Keck Foundation, and J.T.B., in part, by National Institutes of Health Research Service Award I-T32-GM08267. This work is based upon research conducted at the Cornell High Energy Synchrotron Source (CHESS), which is supported by the National Science Foundation under award DMR-9311772, using the Macromolecular Diffraction at CHESS (MacCHESS) facility, which is supported by award RR-01646 from the National Institutes of Health.

References

[1] K. Bloch, Cholesterol: evolution of structure and function, in: D.E. Vance, J.E. Vance (Eds.), Biochemistry of Lipids, Lipoproteins and Membranes, Elsevier, Amsterdam, 1991, pp. 363–381.
[2] Y. Lange, B.V. Ramos, Analysis of the distribution of cholesterol in the intact cell, J. Biol. Chem. 258 (1983) 15130–15134.
[3] M. Bourges, D.M. Small, D.G. Dervichian, Biophysics of lipidic associations. II. The ternary systems cholesterol–lecithin–water, Biochim. Biophys. Acta 137 (1967) 157–167.
[4] H. Lecuyer, D.G. Dervichian, Structure of aqueous mixtures of lecithin and cholesterol, J. Mol. Biol. 45 (1969) 39–57.
[5] C. Horowitz, L. Krut, L. Kaminsky, Cholesterol uptake by egg-yolk phosphatidylcholine, Biochim. Biophys. Acta 239 (1971) 329–336.
[6] R. Freeman, J.B. Finean, Cholesterol:lecithin association at molecular ratios of up to 2:1, Chem. Phys. Lipids 14 (1975) 313–320.
[7] N.L. Gershfeld, Equilibrium studies of lecithin–cholesterol interactions. I. Stoichiometry of lecithin–cholesterol complexes in bulk systems, Biophys. J. 22 (1978) 469–488.
[8] J.J. Collins, M.C. Phillips, The stability and structure of cholesterol-rich codispersions of cholesterol and phosphatidylcholine, J. Lipid Res. 23 (1982) 291–298.
[9] W. Knoll, G. Schmidt, K. Ibel, E. Sackmann, Small-angle neutron scattering study of lateral phase separation in dimyristoylphosphatidylcholine–cholesterol mixed membranes, Biochemistry 24 (1985) 5240–5246.
[10] N. Borochov, E.J. Wachtel, D. Bach, Phase behavior of mixtures of cholesterol and saturated phosphatidylglycerols, Chem. Phys. Lipids 76 (1995) 85–92.
[11] J.J. Cheetham, E. Wachtel, D. Bach, R.M. Epand, Role of the stereochemistry of the hydroxyl group of cholesterol and the formation of nonbilayer structures in phosphatidylethanolamines, Biochemistry 28 (1989) 8928–8934.
[12] D. Bach, N. Borochov, E. Wachtel, Phase separation of

cholesterol in dimyristoyl phosphatidylserine cholesterol mixtures, Chem. Phys. Lipids 92 (1998) 71–77.
[13] J.H. Davis, in: L. Finegold (Ed.), Cholesterol in Membrane Models, CRC Press, Boca Raton, FL, 1993, pp. 67–135.
[14] P.B. Kingsley, G.W. Feigenson, The synthesis of a perdeuterated phospholipid: 1,2-dimyristoyl-sn-glycero-3-phosphocholine-d_{72}, Chem. Phys. Lipids 24 (1979) 135–147.
[15] J.T. Buboltz, G.W. Feigenson, A novel strategy for the preparation of liposomes: rapid solvent exchange, Biochim. Biophys. Acta (in press).
[16] M.W. Tate, E.F. Eikenberry, S.L. Barna, M.E. Wall, J.L. Lowrance, S.M. Gruner, A large-format high-resolution area X-ray detector based on a fiber-optically bonded charge-coupled device (CCD), J. Appl. Cryst. 28 (1995) 196–205.
[17] D.J. Thiel, S.E. Ealick, M.W. Tate, S.M. Gruner, E.F. Eikenberry, Macromolecular crystallographic results obtained using a 2048×2048 CCD detector at CHESS, Rev. Sci. Instrum. 67 (1996) 1–4.
[18] K. Brister, IMP Powder Pattern Circular Integration Program, CHESS, Cornell University, Ithaca, NY, 1997.
[19] G.W. Feigenson, Calcium ion binding between lipid bilayers: The four-component system of phosphatidylserine, phosphatidylcholine, calcium chloride, and water, Biochemistry 28 (1989) 1270–1278.
[20] C.R. Loomis, G.G. Shipley, D.M. Small, The phase behavior of hydrated cholesterol, J. Lipid Res. 20 (1979) 525–535.
[21] B.M. Carven, Crystal structure of cholesterol monohydrate, Nature 260 (1976) 727–729.
[22] H.S. Shieh, L.G. Hoard, C.E. Nordman, Crystal structure of anhydrous cholesterol, Nature 267 (1977) 287–289.
[23] R.S. Bear, K.J. Palmer, F.O. Schmitt, X-ray diffraction studies of nerve lipids, J. Cell Comp. Physiol. 17 (1941) 355–367.
[24] A. Fischer, Elektronenmikroskopie an monomolecularen Lipischichten: Neue Techniken zur Untersuchung der mikroskopischen und molekularen Struktur von reinen und koexistierenden Phasenzustaende, Doctoral Thesis, Technische Universitaet Muenchen, 1984.
[25] M. Caffrey, G.W. Feigenson, Fluorescence quenching in model membranes. 3. Relationship between calcium adenosinetriphosphatase enzyme activity and the affinity of the protein for phosphatidylcholines with different acyl chain characteristics, Biochemistry 20 (1981) 1949–1961.
[26] J.B. Finean, Interaction between cholesterol and phospholipid in hydrated bilayers, Chem. Phys. Lipids 54 (1990) 147–156.
[27] J.R. Green, C. Green, The enrichment of erythrocyte membranes and phosphatidylcholine dispersions with cholesterol, Biochem. Soc. Trans. 1 (1973) 365–368.
[28] J.A. Virtannen, M. Ruonala, M. Vauhkonen, P. Somerharju, Lateral organization of liquid-crystalline cholesterol–dimyristoylphosphatidylcholine bilayers. Evidence for domains with hexagonal and centered rectangular cholesterol superlattices, Biochemistry 34 (1995) 11568–11581.
[29] B.D. Ladbrooke, R.M. Williams, D. Chapman, Studies on lecithin–cholesterol–water interactions by differential scanning calorimetry and X-ray diffraction, Biochim. Biophys. Acta 150 (1968) 333–340.
[30] J. Huang, G.W. Feigenson, A Microscopic interaction model of maximum solubility of cholesterol in lipid bilayers, Biophys. J. (in press).